The Astrophysical Journal Letters, 819:L5 (6pp), 2016 March 1 doi:10.3847/2041-8205/819/1/L5

ON THE 2015 OUTBURST OF THE EXor VARIABLE V1118 ORI

T. Giannini[1], D. Lorenzetti[1], S. Antoniucci[1], A. A. Arkharov[2], V. M. Larionov[2,3], A. Di Paola[1], S. Bisogni[4], and A. Marchetti[5]
[1] INAF—Osservatorio Astronomico di Roma, via Frascati 33, I-00078 Monte Porzio, Italy
[2] Central Astronomical Observatory of Pulkovo, Pulkovskoe shosse 65, 196140 St. Petersburg, Russia
[3] Astronomical Institute of St. Petersburg University, Russia
[4] INAF—Osservatorio Astrofisico di Arcetri, Largo E. Fermi 5, I-50125 Firenze, Italy
[5] INAF—Osservatorio Astronomico di Brera, Via Brera 28, I-20122 Milano, Italy
Received 2016 January 18; accepted 2016 February 9; published 2016 February 23

ABSTRACT

After a long-lasting period of quiescence of about a decade, the source V1118 Ori, one of the most representative members of the EXor variables, is now outbursting. Since the initial increase of the near-infrared flux of about 1 mag (*JHK* bands) registered on 2015 September 22, the source brightness has remained fairly stable. We estimate $\Delta V \sim 3$ mag, with respect to the quiescence phase. An optical/near-IR low-resolution spectrum has been obtained with the Large Binocular Telescope instruments MODS and LUCI2 and compared with a spectrum of a similar spectral resolution and sensitivity level taken during quiescence. Together with the enhancement of the continuum, the outburst spectrum presents a definitely higher number of emission lines, in particular H I recombination lines of the Balmer, Paschen, and Brackett series, along with bright permitted lines of several species, forbidden atomic lines, and CO ro-vibrational lines. Both mass accretion and mass-loss rates have significantly increased (by about an order of magnitude: $\dot{M}_{\rm acc} = 1.2\text{–}4.8\ 10^{-8}\,M_{\odot}\,{\rm yr}^{-1}$, $\dot{M}_{\rm loss} = 0.8\text{–}2\ 10^{-9}\,M_{\odot}\,{\rm yr}^{-1}$), with respect to the quiescence phase. If compared with previous outbursts, the present one appears less energetic. Alternatively, it could already be in the fading phase (with the maximum brightness level reached when the source was not visible), or, viceversa, still in the rising phase.

Key words: accretion, accretion disks – infrared: stars – stars: formation – stars: individual (V1118 Ori) – stars: pre-main sequence – stars: variables: T Tauri, Herbig Ae/Be

1. INTRODUCTION

Last phases of matter accretion of low-to-intermediate mass (0.5–8 $M_{\odot}$) young stellar objects (YSOs) are characterized by magnetospheric accretion events (Shu et al. 1994). Optical and near-IR observations have shown that the accretion process proceeds through irregular and rapid outbursts, with amplitudes in the range of 0.2–1 mag. However, a small percentage of sources, namely the EXor variables (Herbig 1989), undergo much stronger and repetitive outbursts imputed to a sudden increase of the mass accretion rate (e.g., Hartmann & Kenyon 1985, Antoniucci et al. 2008). The typical brightness variation is ∼4–5 mag in the visual band, with a duration from a few months to years and a recurrence time of several years. During the outburst phase, EXor spectra are characterized by emission line spectra, from which accretion rates of $\sim 10^{-6}$–$10^{-8}\,M_{\odot}\,{\rm yr}^{-1}$ are typically estimated (e.g., Lorenzetti et al. 2009; Kóspál et al. 2011; Sicilia-Aguilar et al. 2012; Audard et al. 2014). Such timescale variability makes EXors suitable candidates to perform studies based on evolutionary more-than-statistical concepts aimed at answering the following fundamental questions: (1) what is the mechanism(s) triggering the intermittent accretion bursts?; (2) how does the mass accretion process eventually halt?; (3) what is the role of bursts in the evolution of the circumstellar disk, especially regarding the formation of proto-planetary systems?

The poor characterization of the EXor class derives not only from the small number of known objects (around 20–30 objects, e.g., Lorenzetti et al. 2012; Audard et al. 2014), but also from the lack of a long-term monitoring of the photometric and spectroscopic features of the sources. For these reasons we have started the program EXORCISM (EXOR optiCal and Infrared Systematic Monitoring, Antoniucci et al. 2014), which is based on the 0.3–2.5 μm photometric and spectroscopic monitoring of about 20 objects, classified as EXors or recognized as suitable candidates. Given the cadence of EXor outbursts, quiescence versus outburst phases have been rarely observed with instrumentation having the same performances: as a consequence, the results derived for both states are not meaningfully comparable.

This is not the case of V1118 Ori, an EXor whose long-lasting quiescence phase has been recently investigated (Lorenzetti et al. 2015a, hereafter Paper I) by using an instrumentation similar to that employed for monitoring the outburst presented here. During the last four decades V1118 Ori underwent five outbursts, with an average duration of about a couple of years (1982–84, 1988–90, 1992–94, 1997–98, 2004–06). The first four eruptions are reported by Parsamian et al. (1993), Garcia Garcia & Parsamian (2000), Herbig (2008), and references therein, whereas the properties shown during the fifth event are illustrated by Audard et al. (2005, 2010) and Lorenzetti et al. (2006, 2007). Here we account for the last outburst, which was announced few months ago in a telegram by Lorenzetti et al. (2015b). In Section 2 we describe our optical and near-IR observations, while in Section 3 we analyze and discuss the results. Our concluding remarks are given in Section 4.

2. OBSERVATIONS AND RESULTS

2.1. Near-IR Photometry

Near-IR data were obtained with the 1.1 m AZT-24 telescope at Campo Imperatore (L'Aquila, Italy) equipped with the imager/spectrometer SWIRCAM (D'Alessio et al. 2000),

Table 1
Near-IR Photometry

Date	JD +2400000	*J*	*H* (mag)	*K*
2014 Oct 19	56948.62	12.63	11.57	10.87
2014 Oct 28	56958.63	12.62	11.56	10.79
2014 Nov 01	56962.57	12.52	11.44	10.66
2014 Nov 14	56975.55	12.64	11.61	10.93
2014 Dec 23	57015.47	12.63	11.62	10.95
2015 Jan 15	57038.38	12.63	11.58	10.87
2015 Sep 22	57287.67	11.36	10.67	9.93
2015 Nov 09	57336.55	11.20	10.49	9.70
2015 Nov 12	57339.57	11.38	10.59	9.79
2015 Nov 13	57340.52	11.43	10.61	9.84
2015 Nov 15	57342.54	11.64	10.84	10.04
2015 Nov 17	57344.54	11.49	10.72	9.95
2015 Nov 18	57345.54	11.46	...	...
2015 Nov 19	57346.46	11.44	10.69	9.94
2015 Dec 30	57357.45	11.32	10.60	9.84
2015 Dec 01	57358.48	11.23	10.52	9.76
2015 Dec 02	57359.43	11.42	10.64	9.83
2015 Dec 02	57359.58	11.44	10.68	9.88
2015 Dec 03	57360.47	11.37	10.65	9.87
2015 Dec 04	57361.49	11.49	10.69	9.94
2015 Dec 05	57362.41	11.61	10.79	10.01

Note. Errors on near-IR magnitudes do not exceed 0.03 mag.

which is based on a 256 × 256 HgCdTe PICNIC array. *JHK* photometry was obtained in the period 2015 September–December. Reduction was achieved by using standard procedures for bad pixel cleaning, flat fielding, and sky subtraction. The results are reported in Table 1 and shown in Figure 1. Averaged differences in magnitudes, with respect to the last phase of quiescence (2014 September–October, Paper I), are $\Delta J = 1.23$, $\Delta H = 0.92$, and $\Delta K = 0.99$.

2.2. Optical Spectroscopy

We obtained an optical spectrum with the 8.4 m Large Binocular Telescope (LBT) using the Multi-object Double Spectrograph (MODS—Pogge et al. 2010) on 2015 October 1 and 2 (JD 2 457 296/97). Each of the two observations were performed with the dual grating mode (Blue + Red channels, spectral range 0.35–0.95 μm) and integrated 1500s by using a 0.″8 slit ($\Re \sim 1500$). Each spectral image was independently biased and flat-field corrected, then the sky background was subtracted in the two-dimensional spectral images. The final spectrum was obtained as the average of the two one-dimensional spectra, each obtained by collapsing the stellar trace in the 2D image along the spatial direction. Wavelength calibration was obtained from the spectra of arc lamps, while flux calibration was achieved from observations of spectro-photometric standard stars.

2.3. Near-IR Spectroscopy

A near-IR spectrum of V1118 Ori was obtained with the LUCI2 instrument at LBT on 2015 October 28th (JD 2 457 323). The observations were carried out with the G200 low-resolution grating coupled with the 1.″0 slit. Two data sets were acquired with the standard ABB"A" technique using the *zJ* and *HK* filters, for a total integration time of 12 and 8 minutes, respectively. This provides a final spectrum covering the wavelength range 1.0–2.4 μm at $\Re \sim 1000$. The raw spectral images were flat-fielded, sky-subtracted, and corrected for optical distortions in both the spatial and spectral directions. Telluric absorptions were removed using the normalized spectrum of a telluric standard star, after removal of its intrinsic spectral features. Wavelength calibration was obtained from arc lamps, while flux calibration was based on the photometric data taken in the same span of days. Both optical and near-IR outburst spectra are plotted in Figure 2 together with those obtained during the quiescence phase (taken from Paper I).

3. ANALYSIS AND DISCUSSION

3.1. Photometry

The light curve shown in Figure 1 indicates that after a long period of quiescence that lasted about 10 years, V1118 Ori is currently in a high-level state. Our observations show the beginning of the new outburst between 2015 January and September; in the subsequent three months the source has remained at an approximately constant level. The average near-IR color variation, with respect to the quiescence state, is $\Delta[J - H] = 0.3$ mag, $\Delta[H - K] = -0.06$ mag, which is roughly orthogonal to the extinction vector (see Figure 4 of Paper I). As observed in a number of other classical EXors, this implies that extinction variations, although likely present, do not play a major role during the outburst (see e.g., Figure 1 of Lorenzetti et al. 2012). Indeed, also in the occasion of the 2005 outburst, when the near-IR colors were very similar to the present ones, Audard et al. (2010) did not measure significant extinction variations from the quiescence to the outburst phase. By means of the X-rays column density, they estimated $A_V \sim 1$–2 mag, which are assumed also by us in the present work. A rough estimate of the optical magnitudes has been retrieved from the MODS spectrum. The continuum level increases by a factor between ~40 and 4 passing from *U* to *I* band. Approximate *UBVRI* magnitudes in outburst (quiescence) are $U = 15.8$ (19.8), $B = 15.8$ (19.1), $V = 15.0$ (18.0), $R = 14.2$ (16.9), $I = 13.3$ (14.8). Given that the seeing during the nights of the observations never exceeded 1.″1, no significant flux losses have occurred, so the uncertainties on the estimated magnitudes are below 0.10–0.15 mag. The $[U - B]$, $[B - V]$ colors change from 0.7 and 1.1 mag in quiescence to 0.0 and 0.8 mag in outburst. In previous outbursts, however, the optical colors have become even bluer, being, for example, $[U - B] = -0.84$ and $[U - B] = -0.94$ in 1983 and in 1989 (Parsamian et al. 2002). This fact indicates that the present outburst is one of the least energetic among those observed in V1118 Ori. Indeed, the visual magnitudes registered at the peak of previous outburst have been $V = 13.8$ (1983, Marsden 1984), $V = 12.8$ (1988, Gasparian & Ohanian 1989), $V \leqslant 14.7$ (1992–1994, Garcia Garcia et al. 1995), $V = 13.5$ (1997, Hayakawa et al. 1998), and $V \sim 12.8$ (2005, Audard et al. 2010). However, considering that both the rising and declining times observed in the 1998 and 2005 outbursts have lasted ~100–300 days (Garcia Garcia & Parsamian 2000; Audard et al. 2010), it may be that the maximum level of activity was reached between 2015 January and September (when no observations were available), or that the outburst is still in the rising phase. Very recent observations by Audard et al. (2016) indicate that no significant photometric variations in both optical and near-infrared bands occurred until 2016 mid-January.

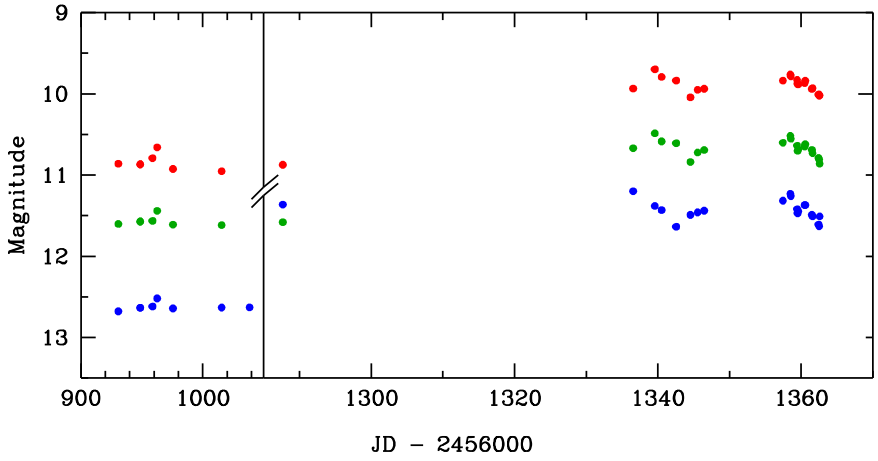

Figure 1. V1118 Ori *JHK* light curve (blue, green, and red, respectively).

3.2. Outburst versus Quiescence Spectrum

The analysis of the optical/near-IR outburst spectrum was essentially done in comparison with the quiescence spectrum discussed in Paper I (shown in Figure 2). This was obtained with a similar instrumental setup as far as spectral resolution and sensitivity level are concerned. Notably, these are one of the few examples of quiescence and outburst spectra of the same source taken with the same high-level instrumentation.

A remarkable number of differences are evidenced by the comparison of the two spectra. (1) A much increased number of emission lines is recognizable in the outburst spectrum, mainly of neutral and ionized metals (H I, He I, Ca II, Fe I, Fe II). Main lines are listed in Table 2 and their fluxes and equivalent widths (EWs) are compared with those measured in the quiescence spectrum (columns 5 and 6). The outburst-to-quiescence flux ratio of the Balmer lines decreases from ∼30 to ∼8 going from $n_{up} = 15$ to $n_{up} = 3$ and that of the Paschen series from ∼30 to ∼12 going from $n_{up} = 12$ to $n_{up} = 7$. Although a detailed modeling of the hydrogen line ratios is far from the aims of this paper, a qualitative comparison with models of Paschen (Edwards et al. 2013) and Balmer (Antoniucci et al. 2016) decrement series suggests that the observed behavior may be explained by a 0.5–0.6 dex increase of the electron density, with no evident dependence on temperature variations. The ratio of the outburst-to-quiescence EW of the Balmer series lines does not depend on n_{up} and is less than unity, suggesting that the line flux increase tightly follows that of the continuum. Conversely, the EW ratios of the Paschen lines are between 2 and 6, indicating that the increase of the continuum level is smaller (and therefore slower) in the infrared than in the optical. The Ca II lines show the largest variations, with $F_{out}/F_{quiesc} \sim 85$ and $EW_{out}/EW_{quiesc} \sim 15$. (2) Forbidden lines of [O I] and [S II], which remained un-detected (or barely detected) in the quiescence spectrum are present in the outburst optical spectrum, suggesting that an enhancement of the mass ejection activity might have been triggered by the increase of the mass accretion rate. (3) A weak Balmer jump (BJ), which is considered a direct indicator of accretion (e.g., Manara et al. 2016 and references therein) is spotted at the end of the Balmer series. We measured the BJ by taking the ratio of the flux at 360 nm to that at 400 nm. We obtained a value of 0.9, more than double the quiescence value. Also, this exceeds the limit of 0.5 empirically put by Herczeg & Hillenbrand (2008) to identify mid-M dwarfs accretors. (4) In the near-IR part of the spectrum, Mg I and Na I in emission, as well as CO overtone emission ($v = 2$–0 and $v = 3$–1), are clearly detected, while they were not present in the quiescence spectrum. (5) Despite the moderate spectral resolution, we are able to detect differences in the spectral profile of the brightest H I lines. As an example, we show in Figure 2 the Hα spectral profile. In the quiescence spectrum, the line is unresolved and the emission peak is close to the rest velocity. During outburst, the line peak is blueshifted by $\approx -70\,km\,s^{-1}$ (with respect to the local standard of rest) with a FWHM $\sim 320\,km\,s^{-1}$, indicating the appearance of a fast wind in this phase. A similar behavior was exhibited by the Hα profile during the 2005 outburst and subsequent decay (Herbig 2008).

3.3. Comparison with Spectra of Previous Outbursts

The 2005 outburst was spectroscopically investigated in the optical and in the near-IR by Herbig (2008) and Lorenzetti et al. (2006), respectively. The optical spectrum was taken by Herbig during the declining phase (2005 November) when the star was somewhat brighter ($V = 14.5$) than at the epoch of our observation. Since the EWs of the most prominent lines (H I, He I, and Ca II; see Herbig 2008's Table 3) were slightly lower than the present ones, we qualitatively deduce that the line fluxes are rather similar in the two outbursts. Herbig (2008) reports the unusual detection of Li I λ6707 *in emission*, a line commonly seen in absorption in classical T Tauri stars. We signal the presence of this line also in the MODS spectrum, although detected at a low signal-to-noise level (Flux $= 1.5 \pm 0.4\ 10^{-15}\,erg\,s^{-1}\,cm^{-2}$).

The near-IR spectrum was taken in 2005 September ($J = 11.2$, Lorenzetti et al. 2006). The same emission features, with similar line fluxes as in the present case, were detected. In particular, since CO emission is believed to originate in the gaseous inner disk where it traces relatively warm (∼4000 K) zones at high densities (Scoville et al. 1980), the constancy of the emitted flux could signal that the physical conditions of the environment around the accretion channels remain similar during all the events, and only the accretion rate varies. Finally, in the same 2005 spectrum, the H_2 1–0S(1) was barely detected. This line appears at around the 1.5σ level also in the LUCI2 spectrum. However, the line, together with the H_2 2–1S (1) line, is definitely detected in the 2D spectral image in a region extending from the source itself up to a distance of ∼17″. The flux ratio between the two lines in such region is ∼2,

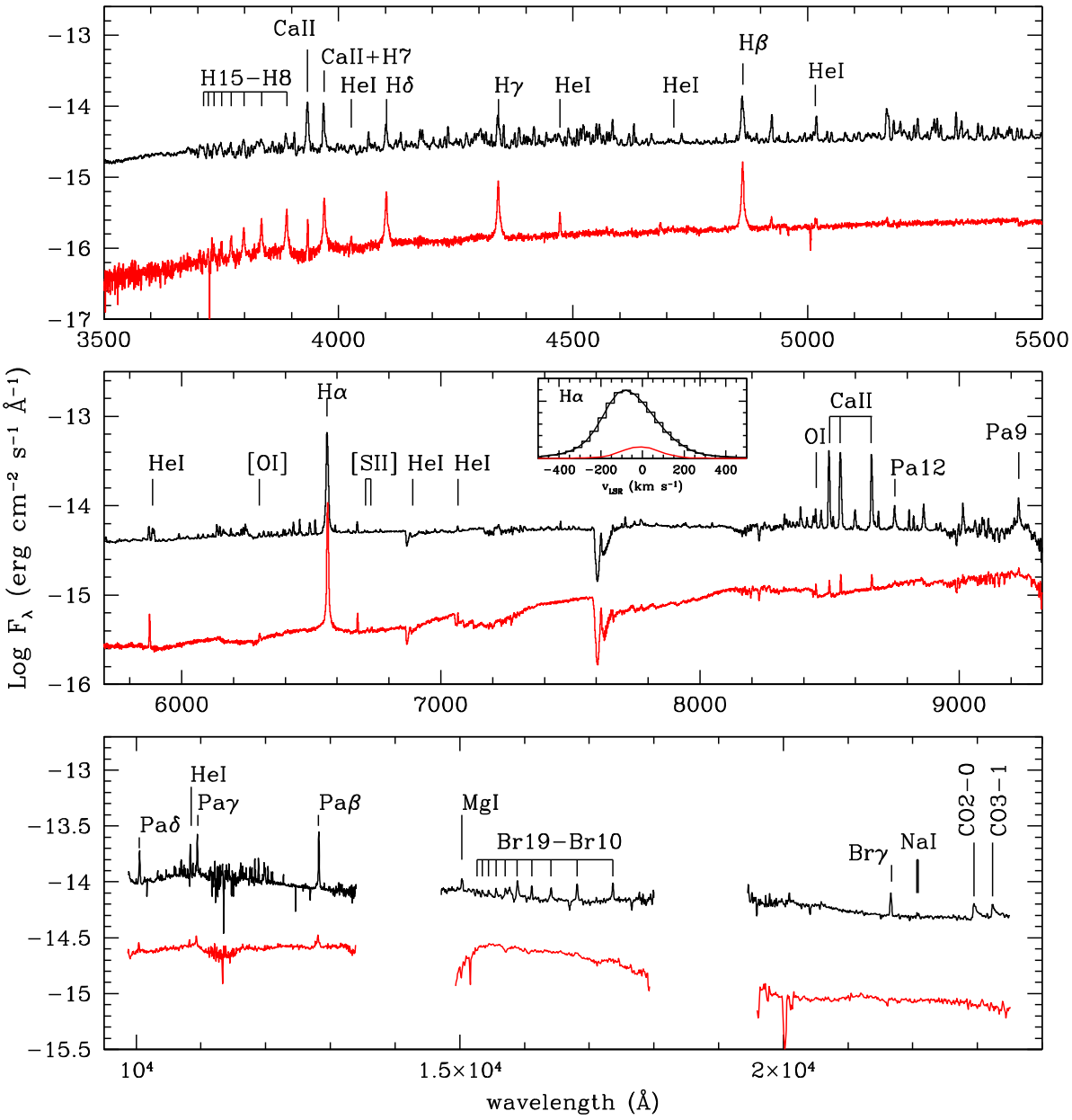

Figure 2. Optical (LBT/MODS) and near-IR (LBT/LUCI2) spectrum of V1118 Ori in the present outburst phase (black) shown in comparison with the quiescence spectrum (red, spectra obtained with LBT/MODS and TNG/NICS, see Paper I). Main emission lines are labeled. Regions corrupted by atmospheric absorption were removed. The inset in the middle panel shows the Hα spectral profile.

suggesting a fluorescent excitation (e.g., Black & van Dishoeck 1987) arising in the nebular environment where the source is located.

3.4. Mass Accretion and Mass-loss Rates

An estimate of the mass accretion rate ($\dot{M}_{\rm acc}$) was obtained from fluxes of bright permitted lines. We employed the relationships between line flux and accretion luminosity ($L_{\rm acc}$) given by Alcalá et al. (2014). For each line, the $L_{\rm acc}$ value was then converted into mass accretion rate ($\dot{M}_{\rm acc}$) by adopting the equation by Gullbring et al. (1998). To have a meaningful comparison with the quiescence phase estimate, we have employed the same lines as in Paper I, namely H I lines of the Balmer and Paschen series along with He I and Ca II bright lines. We also adopted the same parameters as in Paper I, namely: distance of 400 pc, $M_* = 0.4\ M_\odot R_* = 1.29\ R_\odot$ (Hillenbrand 1997; Stassun et al. 1999), and inner radius $R_{\rm in} = 5\ R_\odot$. The result is depicted in Figure 3, where we plot $\dot{M}_{\rm acc}$ for each of the considered lines. The median of the $\dot{M}_{\rm acc}$ values is $1.5\ 10^{-8}\,M_\odot\,{\rm yr}^{-1}$ and $4.2\ 10^{-8}\,M_\odot\,{\rm yr}^{-1}$ if the observed fluxes are de-reddened for $A_V = 1$ and 2 mag, respectively. With the same extinction values, we get $\dot{M}_{\rm acc} = 1$–$3\ 10^{-9}\,M_\odot\,{\rm yr}^{-1}$ in the quiescence state (Paper I).

Assuming that the nearly tenfold enhancement of the [O I] 6300 flux is due to an increase of the mass ejection activity, we derived mass ejection rates $\dot{M}_{\rm loss} = 0.8\ 10^{-9}\,M_\odot\,{\rm yr}^{-1}$ and $2.0\ 10^{-9}\,M_\odot\,{\rm yr}^{-1}$ for $A_V = 1$ and 2 mag, respectively, following the relationship given by Hartigan et al. (1994). The same model gives $0.8\ 10^{-10}\,M_\odot\,{\rm yr}^{-1}$ and $2.0\ 10^{-10}\,M_\odot\,{\rm yr}^{-1}$ for the quiescence phase. It is of interest to compare the ratio $\dot{M}_{\rm acc}/\dot{M}_{\rm loss}$ in the two phases; while this ratio is ∼13 in

Table 2
Main Lines Detected in V1118 Ori

Line ID	λ_{air} (Å)	Flux $\pm$ Δ(Flux) (10^{-15} erg s^{-1} cm^{-2})	EW (Å)	F_{out}/F_{quiesc}	EW_{out}/EW_{quiesc}
		LBT-MODS			
H15	3711.97	2.8 $\pm$ 0.3	−1.4	31 $\pm$ 13	0.8
H14	3721.94	3.1 $\pm$ 0.3	−1.4	34 $\pm$ 14	0.9
H13	3734.37	4.3 $\pm$ 0.4	−2.0	48 $\pm$ 20	1.4
H12	3750.15	4.8 $\pm$ 0.4	−2.1	30 $\pm$ 8	0.9
H11	3770.63	5.3 $\pm$ 0.4	−2.5	16 $\pm$ 3	0.5
H10	3797.90	7.5 $\pm$ 0.4	−3.5	15 $\pm$ 2	0.5
H9	3835.38	9.0 $\pm$ 0.4	−3.9	10 $\pm$ 1	0.4
H8	3889.05	8.7 $\pm$ 0.4	−3.7	7 $\pm$ 1	0.3
Ca II K	3933.66	41.2 $\pm$ 0.4	−18.0	91 $\pm$ 5	3.0
Ca II+H7	3968.45/3970.07	40.0 $\pm$ 0.4	−17.4	17 $\pm$ 1	0.7
He I	4026.2	3.2 $\pm$ 0.4	−1.5	18 $\pm$ 5	0.9
Hδ	4101.73	22.5 $\pm$ 0.4	−9.6	8 $\pm$ 1	0.4
Hγ	4340.46	26.0 $\pm$ 0.4	−9.1	6.0 $\pm$ 0.2	0.3
He I	4471.5	2.0 $\pm$ 0.4	−0.7	7 $\pm$ 2	0.2
He I	4713.2	0.9 $\pm$ 0.4	−0.3	10 $\pm$ 6	0.6
Hβ	4861.32	59.9 $\pm$ 0.4	−18.5	9.0 $\pm$ 0.2	0.5
He I	5015.67	4.1 $\pm$ 0.4	−1.2	24 $\pm$ 5	1.3
He I	5875.6	7.3 $\pm$ 0.4	−2.3	7 $\pm$ 1	0.4
[O I]	6300.30	3.4 $\pm$ 0.4	−0.8	11 $\pm$ 3	0.8
Hα	6562.80	470.3 $\pm$ 0.4	−94.6	8.0 $\pm$ 0.1	0.8
He I	6678.15	7.4 $\pm$ 0.4	−1.5	8 $\pm$ 1	0.7
[S II]	6716.44	1.3 $\pm$ 0.4	−0.3	4 $\pm$ 2	0.5
[S II]	6730.81	<1.2	...	<3.5	...
He I	7065.2	5.4 $\pm$ 0.4	−1.0	8 $\pm$ 3	0.7
O I	8446.5	18.3 $\pm$ 0.4	−3.2	12 $\pm$ 2	2.0
Ca II	8498.03	187.6 $\pm$ 0.4	−33.1	83 $\pm$ 4	14.4
Ca II	8542.09	208.6 $\pm$ 0.4	−36.6	84 $\pm$ 2	15.9
Ca II	8662.14	191.1 $\pm$ 0.4	−34.8	92 $\pm$ 4	19.3
Pa12	8750.47	33.8 $\pm$ 0.4	−6.1	28 $\pm$ 5	6.7
Pa9	9229.01	60.1 $\pm$ 0.4	−11.7	25 $\pm$ 9	7.9
		LBT-LUCI2			
Paδ	10049.37	135 $\pm$ 10	−14	16 $\pm$ 3	4.7
He I	10830.3	118 $\pm$ 10	−11	17 $\pm$ 3	4.5
Paγ	10938.09	212 $\pm$ 10	−19	20 $\pm$ 3	4.4
Paβ	12818.08	323 $\pm$ 10	−29	12 $\pm$ 32	2.1
Mg I	15029/15051	71 $\pm$ 7	−8	>11	...
Br19	15264.71	30 $\pm$ 7	−4	>6	...
Br18	15345.98	32 $\pm$ 7	−4	>6	...
Br17	15443.14	35 $\pm$ 7	−5	>7	...
Br16	15560.70	37 $\pm$ 7	−6	>6	...
Br15	15704.95	41 $\pm$ 7	−6	>8	...
Br14+O I	15885/15892	86 $\pm$ 7	−12	>14	...
Br13	16113.71	54 $\pm$ 7	−8	>9	...
Br12	16411.67	62 $\pm$ 7	−9	>10	...
Br11	16811.11	72 $\pm$ 7	−11	>12	...
Br10	17366.85	75 $\pm$ 7	−11	>12	...
Brγ	21655.29	78 $\pm$ 6	−16	>13	...
Na I	22062.4	7 $\pm$ 1	−1.5	>1.2	...
Na I	22089.7	9 $\pm$ 1	−2	>1.5	...
CO 2–0	22943	158 $\pm$ 1	−34	>26	...
CO 3–1	23235	142 $\pm$ 1	−30	>24	...

Note. Upper limits are computed at 3σ level.

quiescence, it increases to ∼18 during the outburst. Although the difference is slight, this indicates that the enhancement of the mass ejection rate proceeds more slowly than that of the mass accretion rate.

Finally, to compare the mass accretion rate in two subsequent outbursts, we applied the procedure described above to the fluxes reported in Lorenzetti et al. (2006). We get $\dot{M}_{acc}(2005) \sim 10^{-7}\,M_{\odot}\,yr^{-1}$, namely about a factor 5–10 larger than the present value. However, such an estimate is based only on near-IR line fluxes, which, as can been seen in Figure 3, tend to give higher values than the optical lines. In this sense, the value of $\dot{M}_{acc}(2005)$ has to be considered as an upper limit.

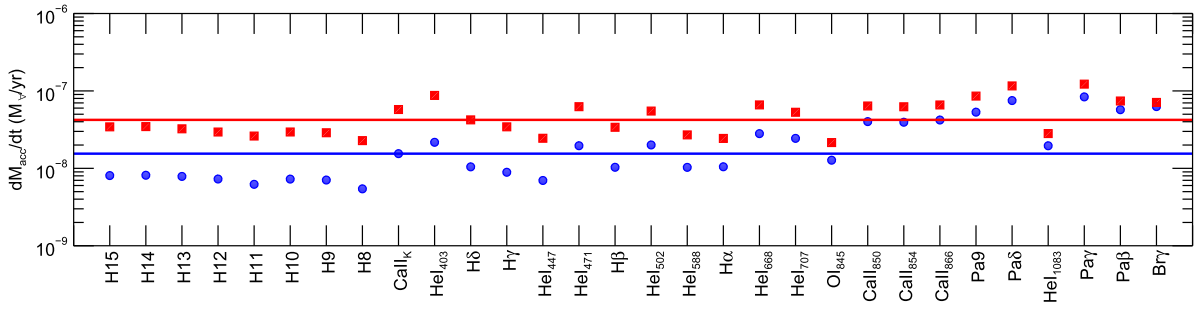

Figure 3. Mass accretion rate determination computed from the flux of the labeled tracers using Alcalá et al. (2014) relationships. The assumed visual extinction is $A_V = 1$ mag (blue circles) and $A_V = 2$ mag (red squares). The median $\dot{M}_{\rm acc}$ values are marked for both cases with a solid line.

Alternatively, this might indicate that the present outburst is weaker than the previous one or that the observed brightness is not at its maximum level.

4. CONCLUDING REMARKS

We have detected a new outburst of the EXor variable V1118 Ori, and obtained the optical and near-IR low-resolution spectra. These have been analyzed in comparison to the quiescence ones, which were acquired with a very similar instrumental setup. The main results of our study are:

1. we registered an increase of the continuum level. This increase goes from a factor ∼40 in U band down to factor ∼4 from I to K bands;
2. the outburst spectrum is rich in emission lines, mainly from neutral and ionized metals. In particular, the fluxes of H I recombination lines have increased by about an order of magnitude;
3. an increase of about an order of magnitude is estimated in the mass accretion rate. From bright optical and near-IR lines we estimate $\dot{M}_{\rm acc} = 1.2$–$4.8\ 10^{-8}\,M_\odot\,{\rm yr}^{-1}$.
4. A few forbidden lines from O I and S II are detected, likely indicating an enhancement of the mass ejection activity that is associated with the increase of the accretion rate. From the [O I]6300 luminosity we estimate $\dot{M}_{\rm loss} = 0.8$–$2\ 10^{-9}\,M_\odot\,{\rm yr}^{-1}$.
5. A comparison with light curves of previous outbursts suggests that the present outburst is relatively weak. Alternatively, it may be that the maximum level of the outburst activity was reached between January and September 2015 (when no observations are available), or that the outburst is still in the rising phase.

This research was based on observations made with different instruments. (1) The Large Binocular Telescope (LBT) is an international collaboration among institutions in the United States, Italy, and Germany. LBT Corporation partners are the University of Arizona on behalf of the Arizona University system; Istituto Nazionale di Astrofisica, Italy; LBT Beteiligungsgesellschaft, Germany, representing the Max-Planck Society, the Astrophysical Institute Potsdam, and Heidelberg University; The Ohio State University, and The Research Corporation, on behalf of The University of Notre Dame, University of Minnesota, and University of Virginia. (2) The AZT-24 IR Telescope at Campo Imperatore (L'Aquila—Italy) operated under the responsability of the INAF-Osservatorio Astronomico di Roma (OAR). V.L. acknowledges support from St. Petersburg University research grant 6.38.335.2015.

REFERENCES

Alcalá, J. M., Natta, A., Manara, C. F., et al. 2014, A&A, 561, 2
Antoniucci, S., Arkharov, A. A., Di Paola, A., et al. 2014, A&A, 565, L7
Antoniucci, S., Nisini, B., Giannini, T., & Lorenzetti, D. 2008, A&A, 479, 503
Antoniucci, S., Rigliaco, E., Nisini, B., et al. 2016, A&A, submitted
Audard, M., Ábrahám, P., Dunham, M. M., et al. 2014, in Protostars and Planets VI, ed. H. Beuther et al. (Tucson, AZ: Univ. Arizona Press), 387
Audard, M., Güdel, M., Skinner, S. L., et al. 2005, ApJL, 635, L81
Audard, M., Hamaguchi, K., Kastner, J., Grosso, N., & Walter, F. M. 2016, ATel, 8548
Audard, M., Stringfellow, G. S., Güdel, M., et al. 2010, A&A, 511, 63
Black, J. H., & van Dishoeck, E. F. 1987, ApJ, 322, 412
D'Alessio, F., Di Cianno, A., Di Paola, A., et al. 2000, Proc. SPIE, 4008, 748
Edwards, S., Kwan, J., Fischer, W., et al. 2013, ApJ, 778, 148
Garcia Garcia, J., Mampaso, A., & Parsamian, E. S. 1995, IBVS, 4268, 1
Garcia Garcia, J., & Parsamian, E. S. 2000, IBVS, 4925, 1
Gasparian, K. G., & Ohanian, G. B. 1989, IBVS, 3327, 1
Gullbring, E., Hartmann, L., Briceño, C., & Calvet, N. 1998, ApJ, 492, 323
Hartigan, P., Morse, J. A., & Raymond, J. 1994, ApJ, 436, 125
Hartmann, L., & Kenyon, S. J. 1985, ApJ, 299, 462
Hayakawa, T., Ueda, T., Uemura, M., et al. 1998, IBVS, 4615, 1
Herbig, G. H. 1989, in European Southern Observatory Conf. and Workshop Proc. 33, 233
Herbig, G. H. 2008, AJ, 135, 637
Herczeg, G. J., & Hillenbrand, L. A. 2008, ApJ, 681, 594
Hillenbrand, L. A. 1997, AJ, 113, 1733
Kóspál, Á, Ábrahám, P., Acosta-Pulido, J. A., et al. 2011, A&A, 527, A133
Lorenzetti, D., Antoniucci, S., Giannini, T., et al. 2012, ApJ, 749, 188
Lorenzetti, D., Antoniucci, S., Giannini, T., et al. 2015a, ApJ, 802, 24 (Paper I)
Lorenzetti, D., Arkharov, A. A., Di Paola, A., et al. 2015b, ATel, 8100
Lorenzetti, D., Giannini, T., Calzoletti, L., et al. 2006, A&A, 453, 579
Lorenzetti, D., Giannini, T., Larionov, V. M., et al. 2007, ApJ, 665, 1182
Lorenzetti, D., Larionov, V. M., Giannini, T., et al. 2009, ApJ, 693, 1056
Manara, C. F., Fedele, D., Herczeg, G. J., & Teixeira, P. S. 2016, A&A, 585, 136
Marsden, B. G. 1984, IAUC, 3924, 1
Parsamian, E. S., Ibragimov, M. A., Oganyan, G. B., & Gasparyan, K. G. 1993, Ap, 36, 12
Parsamian, E. S., Mujica, R., & Corral, L. 2002, Ap, 45, 393
Pogge, R. W., Atwood, B., Brewer, D. F., et al. 2010, Proc. SPIE, 7735, 77350A
Scoville, N. Z., Krotkov, R., & Wang, D. 1980, ApJ, 240, 929
Shu, F. H., Najita, J., Ruden, S. P., & Lizano, S. 1994, ApJ, 429, 797
Sicilia-Aguilar, A., Kóspál, Á, Setiawan, J., et al. 2012, A&A, 544, 93
Stassun, K. G., Mathieu, R. D., Mazeh, T., & Vrba, F. J. 1999, AJ, 117, 2941